Isotope effects in the harmonic response from hydrogenlike muonic atoms in strong laser fields

Atif Shahbaz,[1,*] Thomas J. Bürvenich,[2] and Carsten Müller[1,†]
[1]*Max-Planck-Institut für Kernphysik, Saupfercheckweg 1, D-69117 Heidelberg, Germany*
[2]*Frankfurt Institute for Advanced Studies, Johann Wolfgang Goethe University, Ruth-Moufang-Strasse 1, D-60438 Frankfurt am Main, Germany*
(Received 14 February 2010; published 27 July 2010)

High-order harmonic generation from hydrogenlike muonic atoms exposed to ultraintense high-frequency laser fields is studied. Systems of low nuclear-charge number Z are considered where a nonrelativistic description applies. By comparing the radiative response for different isotopes, we demonstrate characteristic signatures of the finite nuclear mass and size in the harmonic spectra. In particular, for $Z > 1$, an effective muon charge appears in the Schrödinger equation for the relative particle motion, which influences the position of the harmonic cutoff. Cutoff energies in the million-electron-volt domain can be achieved, offering prospects for the generation of ultrashort coherent γ-ray pulses.

DOI: 10.1103/PhysRevA.82.013418 PACS number(s): 42.65.Ky, 36.10.Ee, 21.10.−k

I. INTRODUCTION

One of the most successful and accurate methods to probe nuclear properties employs muonic atoms [1]. Due to the small Bohr radius of these exotic atoms, the muonic wave function has a large overlap with the binding nucleus. Precision measurements of muonic transitions to deeply bound states can therefore reveal information on nuclear structure such as finite size, deformation, surface thickness, and polarization. The first x-ray spectroscopy of muonic atoms was performed in 1953 using a four-meter cyclotron [2]. Today, large-scale facilities such as TRIUMF (Vancouver, Canada) or the Paul Scherrer Institute, PSI (Villigen, Switzerland) exist which are specialized in the efficient generation of muons and muonic atoms [3]. New developments aim at the production of radioactive muonic isotopes for conducting spectroscopic studies on unstable nuclear species [4]. Muons bound in atoms are also able to catalyze nuclear fission [5] and fusion [6] reactions.

On a different front, the field of laser-nuclear physics is emerging [7]. While lasers have always represented important tools for nuclear spectroscopy [8], in recent years their role is qualitatively changing and growing because of the tremendous progress in high-power laser technology. The interaction of intense short laser pulses ($I \sim 10^{18}$–10^{20} W/cm^2) with matter can produce highly energetic electrons, protons, and photons (e.g., via bremsstrahlung). In pioneering experiments, this has led to the observation of laser-induced nuclear fission [9], nuclear fusion [10], and neutron production in nuclear reactions [11]. Advanced laser sources might also pave the way to nuclear quantum optics [12] and coherent γ spectroscopy using ultrashort pulses [13–15].

In light of this, the combination of muonic atoms with intense laser fields opens promising perspectives. Contrary to the traditional spectroscopy of muon transitions between stationary bound states, the exposure of a muonic atom to a strong laser field renders the problem explicitly time dependent and thus makes the muon a *dynamic* nuclear probe. In this setup, the muon is coherently driven across the nucleus, which, for example, gives rise to the emission of radiation and, in general, allows for time-resolved studies on a femtosecond scale. The information on the nucleus gained by laser assistance can in principle complement the knowledge obtained from the usual field-free spectroscopy of muonic atoms.

Against this background, we have recently considered the process of high-harmonic generation (HHG) from strongly laser-driven muonic hydrogen and deuterium atoms [16]. The process of HHG represents a frequency up-conversion of the applied laser frequency due to a nonlinear coupling of the atom with the driving external field (see [17–20] for recent reviews). It can be understood within a three-step model, where the bound lepton is liberated from the atom by tunneling ionization, propagates in the laser field, and finally recombines with the core, returning its kinetic energy upon photoemission. By way of a comparative study, it was demonstrated that the harmonic response from muonic hydrogen isotopes is sensitive to the nuclear mass and size [16]. This shows that muonic atoms subject to strong laser fields can reveal information on nuclear degrees of freedom. Muonic deuterium molecules in superintense laser fields represent another interesting example toward this combined effort, where field-induced modifications of muon-catalyzed fusion have been investigated [21]. Moreover, muonic hydrogen atoms have been studied as systems, which could allow for observation of the Unruh effect [22].

In this article, we extend our previous study on HHG [16] to hydrogenlike muonic atoms (ions) with nuclear-charge number $Z \geqslant 1$. To this end, the time-dependent Schrödinger equation describing the muon in the presence of the binding nucleus and a strong laser field is considered. Characteristic isotope effects arising from the finite nuclear mass and size are found. Moreover, in the case $Z > 1$, the laser-driven particle dynamics becomes more complex because the center of mass of the atomic constituents does not stay at rest any longer. As a result, an effective muon charge appears in the Schrödinger equation for the relative motion, which affects the harmonic cutoff position. The cutoff energies achievable with muonic atoms in the nonrelativistic domain of interaction are very large, reaching several million electron volts. This holds in

*Permanent address: Department of Physics, GC University, 54000 Lahore, Pakistan.
†c.mueller@mpi-k.de

principle prospects for the production of coherent γ-ray pulses of ultrashort duration (see also [23]).

Since muonic atoms are tightly bound systems, laser fields of extraordinary field strength and photon energy are required to influence the muon motion. In the ground state of muonic hydrogen, for example, the muon is bound by 2.5 keV and experiences a binding Coulomb field strength of 1.8×10^{14} V/cm corresponding to the field intensity 4.2×10^{25} W/cm^2. A comparison of these numbers with the parameters of the most advanced present-day and near-future laser sources is useful. In the range of optical and near-infrared frequencies ($\hbar\omega \sim 1$ eV), the highest intensity presently attainable is $\sim 10^{22}$ W/cm^2 [24] and the next generation of high-power lasers aims at intensities of 10^{23} W/cm^2 and beyond [25]. In the vacuum ultraviolet (VUV) frequency domain ($\hbar\omega \sim$ 10–100 eV), a maximum intensity of $\sim 10^{17}$ W/cm^2 has been attained with a free-electron laser at the FLASH facility (DESY, Germany) [26]. The Linac Coherent Light Source (SLAC, Stanford) has recently entered the frequency domain $\hbar\omega \sim 1$ keV [27]. Near-future upgrades of such machines are planned to produce brilliant x-ray beams ($\hbar\omega \sim 10$ keV) with peak intensities close to 10^{20} W/cm^2. There are also efforts to generate ultrashort, high-frequency radiation ($\hbar\omega \sim$ 10–1000 eV) from plasma surface harmonics where considerably higher intensities might be reachable due to a high conversion efficiency [28]. With these novel sources of intense coherent radiation, it will become possible to influence the quantum dynamics of light muonic atoms with nuclear-charge numbers $Z \lesssim 10$.

As to their lifetime, we point out that light muonic atoms and molecules may be regarded as quasistable systems on the ultrashort time scales of strong laser pulses ($\tau \sim$ fs–ps), since their lifetime is determined by the free muon lifetime of 2.2 μs. For the field parameters assumed in this article, the influence of the external laser field on the muon decay is immaterial as well [29]. In deeply bound states of heavy atoms, the muon lifetime can be reduced due to absorption by the nucleus to $\sim 10^{-8}$ s which still exceeds typical laser pulse durations by orders of magnitude.

We organize the article as follows: Sec. II deals with the theoretical framework in which the separation into center of mass and relative coordinates of the two-body Schrödinger equation for a hydrogenlike muonic atom in a laser field is performed. We also give here a scaling transformation between ordinary and muonic atoms. Section III has been reserved for the presentation of our analytical and numerical results. Section III A compiles the harmonic cutoff energies available from different low-Z muonic atoms. Section III B treats the influence of the nuclear mass on the position of the harmonic cutoff. Section III C shows a series of numerical calculations devoted to the impact of the nuclear size on the HHG spectra. A comparison of the nuclear signatures predicted for muonic atoms with those to be expected in highly charged electronic ions is undertaken in Sec. III D. The conclusion is given in Sec. IV.

II. THEORETICAL FRAMEWORK

A. Separation of relative and center-of-mass motion

We consider the nonrelativistic quantum dynamics of an initially bound muon in a few-cycle laser pulse described by the time-dependent Schrödinger equation (TDSE). For our laser parameters of interest, we may ignore the space dependence of the laser field (dipole approximation), treating it as a purely time-dependent electric field. Due to the large muon mass, the atomic nucleus cannot be considered as infinitely heavy. We therefore start from the two-particle TDSE written in the length gauge as

$$i\hbar\frac{\partial}{\partial t}\psi(\mathbf{x}_\mu,\mathbf{x}_n;t) = \left[\frac{\mathbf{p}_\mu^2}{2m_\mu}+\frac{\mathbf{p}_n^2}{2m_n} + e\mathbf{x}_\mu\cdot\mathbf{E}(t) - Ze\mathbf{x}_n\cdot\mathbf{E}(t) + V(|\mathbf{x}_\mu-\mathbf{x}_n|)\right]\psi(\mathbf{x}_\mu,\mathbf{x}_n;t), \quad (1)$$

where m_μ and m_n are the muonic and nuclear masses, $\mathbf{x}_\mu$ and $\mathbf{x}_n$ are the coordinate vectors for the muon and the nucleus, and $\mathbf{p}_\mu = -i\hbar\partial/\partial\mathbf{x}_\mu$ and $\mathbf{p}_n = -i\hbar\partial/\partial\mathbf{x}_n$ are the corresponding momentum operators, respectively. Besides, the nuclear-charge number is Z, the elementary charge unit is e, the binding potential is $V(|\mathbf{x}_\mu - \mathbf{x}_n|)$, and the laser electric field is $\mathbf{E}(t)$, which oscillates with angular frequency ω.

The application of the dipole approximation in Eq. (1) considerably simplifies the problem as it renders the Schrödinger equation (1) for the muon-nucleus two-body system separable into relative and center-of-mass motion. By introducing relative and center-of-mass coordinates $\mathbf{x} = \mathbf{x}_\mu - \mathbf{x}_n$ and $\mathbf{X} = (m_\mu\mathbf{x}_\mu + m_n\mathbf{x}_n)/M$, respectively, with the total mass $M = m_\mu + m_n$, one finds that the evolution of the center of mass is described by

$$i\hbar\frac{\partial}{\partial t}\Psi(\mathbf{X},t) = \left[\frac{\mathbf{P}^2}{2M} - (Z-1)e\mathbf{X}\cdot\mathbf{E}(t)\right]\Psi(\mathbf{X},t), \quad (2)$$

with $\mathbf{P} = -i\hbar\partial/\partial\mathbf{X}$. Equation (2) is the nonrelativistic Volkov equation for a particle of charge $(Z-1)e$ and mass M in the presence of a laser field. As a consequence, the center-of-mass motion does not emit higher harmonic frequencies and may therefore be ignored in the following. Note that in the special case $Z = 1$ (i.e., hydrogen isotopes) the center of mass moves freely, while the laser field couples only to the relative coordinate [30].

The relative motion is governed by (see also [21,31])

$$i\hbar\frac{\partial}{\partial t}\psi(\mathbf{x},t) = \left[\frac{\mathbf{p}^2}{2m_r} + q_e\mathbf{x}\cdot\mathbf{E}(t) + V(\mathbf{x})\right]\psi(\mathbf{x},t), \quad (3)$$

with the reduced mass $m_r = m_\mu m_n/M$, the relative momentum $\mathbf{p} = -i\hbar\partial/\partial\mathbf{x}$, and the effective charge

$$q_e = m_r\left(\frac{Z}{m_n}+\frac{1}{m_\mu}\right)e. \quad (4)$$

In the special case of $Z = 1$, the effective charge reduces to $q_e = e$, whereas $q_e > e$ holds for atomic numbers $Z > 1$.

Formally, Eq. (3) is the Schrödinger equation for a single particle of charge $-q_e$ and mass m_r in the presence of a nucleus and a laser field. The accelerated motion of the relative coordinate in the combined external fields therefore gives rise to the emission of higher harmonics. We note that, in physical terms, the relative coordinate accounts for the fact that both the nucleus and the muon oscillate in the laser field with different amplitudes in opposite directions (see also Fig. 2 in [16]).

We point out that the effective charge in Eq. (4) has already been derived in Ref. [32]. It was also shown there that the two-body TDSE in a laser field separates straightforwardly in the velocity gauge. It is interesting to note that, in contrast, the separability in the length gauge is a more subtle issue because the operations of performing gauge transformations and dipole approximations are not commutative [32,33]. As a consequence, cross terms appear in the exact version of the two-body TDSE in the length gauge, which, strictly speaking, prevent the equation from being separable. The cross terms typically become important at the borderline to the relativistic regime when the value of the relativistic field parameter [see Eq. (9)] approaches unity [32]. For the nonrelativistic laser parameters applied in the present study, however, these terms are very small and have therefore been neglected in Eq. (1).

B. Scaling considerations

The form of Eq. (3) is equivalent to the Schrödinger equation for an ordinary hydrogen atom (i.e., an electron bound to an infinitely heavy proton) in a laser field. The relation can be made explicit by virtue of a general method known as scaling transformation. For the special case of a laser-driven atom, the scaling procedure is nicely explained in [31]. Suppose, that we have a hydrogenlike muonic system of nuclear charge Z on the one side and an ordinary hydrogen atom on the other side. We introduce an electronic coordinate vector $\mathbf{x}_e$ and time t_e and relate them to the muonic coordinate $\mathbf{x}$ and time t of Eq. (3) according to

$$\mathbf{x}_e = \frac{Z}{\rho}\mathbf{x}; \quad t_e = \frac{Z^2}{\rho}t, \tag{5}$$

with the mass ratio $\rho \equiv m_e/m_r$ and the electron mass m_e. When rewritten in the scaled space and time, Eq. (3) becomes

$$i\hbar\frac{\partial}{\partial t_e}\psi(\mathbf{x}_e,t_e) = \left[\frac{\mathbf{p}_e^2}{2m_e} + e\mathbf{x}_e\cdot\mathbf{E}_e(t_e) + V(\mathbf{x}_e)\right]\psi(\mathbf{x}_e,t_e), \tag{6}$$

with $\mathbf{p}_e = -i\hbar\partial/\partial\mathbf{x}_e$ and the scaled laser frequency and field strength

$$\omega_e = \frac{\rho}{Z^2}\omega; \quad \mathbf{E}_e = \frac{q_e}{e}\frac{\rho^2}{Z^3}\mathbf{E}. \tag{7}$$

This means that a muonic hydrogenlike atom in a laser field with parameters E and ω behaves like an ordinary hydrogen atom in a field with E_e and ω_e given by Eq. (7), provided that the binding potential $V(x)$ arises from a pointlike nucleus. To give an example, the typical parameters of an intense Ti:sapphire laser $\hbar\omega_e = 1.5$ eV, $E_e = 2.7\times10^8$ V/cm (10^{14} W/cm^2), translate to a muonic helium atom as $\hbar\omega = 1.2$ keV, $E = 9.1\times10^{13}$ V/cm (1.1×10^{25} W/cm^2). This comparison demonstrates that despite the huge laser intensities applied in our computations, the laser-driven muon dynamics remains nonrelativistic due to the large muon mass. Moreover, since the laser intensities required for HHG from muonic atoms are very large already for hydrogen isotopes and steeply increase with the nuclear charge, we restrict our consideration to muonic atoms with $Z \lesssim 10$. An advantage of these systems as compared to heavier ones is that the relative differences in mass and size among isotopes are larger for low-Z atoms in the nuclear chart.

We emphasize that the scaling procedure does not account for nuclear properties like the finite nuclear size or the nuclear shape. Evidently, when the transition from, for example, a muonic hydrogen atom to an ordinary hydrogen atom is performed, the proton radius is not to be length scaled in accordance with Eq. (5) but remains fixed. As a consequence, for atomic systems where nuclear properties play a role, not all physical information can be obtained from the knowledge of the ordinary-atom case via scaling. In Sec. III C, we show results which display the influence of the nuclear size on the process of HHG.

III. RESULTS

Based on Eq. (3), we demonstrate in the following various isotope effects in the HHG spectra of muonic atoms. By analytical means, the harmonic cutoff position is shown to depend on the nuclear mass via the reduced mass of the two-body system and the effective muon charge; these findings are illustrated by numerically computed HHG spectra. Numerical calculations within an approximate model are used moreover to provide indications that the harmonic plateau height depends in addition on the nuclear size. The nuclei chosen for the calculations are given in Table I.

To begin, let us give a general consideration of the laser field parameters required and the maximum cutoff energies attainable from muonic atoms.

A. Maximum cutoff energies

Since the conversion efficiency into high harmonics is rather low ($\sim10^{-6}$), it is generally desirable to maximize the radiative signal strength. In our situation, the optimization is of particular importance as the target density of muonic atoms is low. A sizable HHG signal requires efficient ionization on the one hand, as well as efficient recombination on the other hand. The former is guaranteed if the laser peak field strength lies just below the border of overbarrier ionization (OBI) where the Coulomb barrier is suppressed all the way to the bound energy level by the laser field [19]. From Eq. (3), we obtain

$$E \lesssim E^{\mathrm{OBI}} = \frac{m_r^2c^3}{q_e\hbar}\frac{(\alpha Z)^3}{16}, \tag{8}$$

TABLE I. Nuclear masses and rms charge radii of various isotopes which have been used in the calculations. The half-lives of ^{9}Li and ^{23}Ne amount to 178 ms and 37 s, respectively; the other nuclei are stable.

Isotope	Mass m_n (GeV/c^2)	Ref.	Size R (fm)	Ref.
H	0.9383	[34]	0.875	[35]
D	1.8756	[34]	2.139	[35]
^{3}He	2.8084	[34]	1.9448	[36]
^{4}He	3.7274	[34]	1.6757	[36]
^{6}Li	5.6016	[34]	2.517	[37]
^{9}Li	8.4069	[34]	2.217	[37]
^{20}Ne	18.493	[38]	3.0053	[36]
^{23}Ne	21.277	[38]	2.9126	[36]

with the fine-structure constant $\alpha \approx 1/137$ and the speed of light c. Efficient recollision is guaranteed if the magnetic drift along the laser propagation direction can be ignored, which limits the relativistic parameter to [39,40]

$$\xi \equiv \frac{q_e E}{m_r c \omega} < \left(\frac{16\hbar\omega}{\sqrt{2 m_r c^2 I_p}} \right)^{1/3}. \tag{9}$$

Here, I_p denotes the atomic ionization potential. The condition (9) also confirms the applicability of the dipole approximation in Eq. (3).

The Eqs. (8) and (9) define a maximum laser intensity $I_{\max} \approx I^{\mathrm{OBI}}$ and a minimum laser frequency

$$\omega_{\min} = \frac{m_r c^2}{16\hbar} (\alpha Z)^{5/2}, \tag{10}$$

which are still in accordance with the conditions imposed. At these laser parameters, the maximum harmonic cutoff energies are attained, while Eqs. (8) and (9) guarantee an efficient ionization-recollision process. Note, however, that smaller driving frequencies generally lead to reduced harmonic signal strengths because of the more pronounced and unavoidable quantum wave-packet spreading [41–43] (for an exception to this rule, see [44]). For muonic hydrogen, the lowest frequency according to Eq. (10) lies in the VUV range, $\hbar\omega_{\min} \approx 27$ eV, while the maximum field intensity is $I^{\mathrm{OBI}} \approx 1.6 \times 10^{23}$ W/cm^2. At these values, the harmonic spectrum extends to a maximum energy of $\epsilon_{\max} = I_p + 3.17 U_p \approx 0.55$ MeV, where U_p is the ponderomotive energy [see Eqs. (11) and (12)]. For light muonic atoms with nuclear-charge number $Z > 1$, the achievable cutoff frequencies are even higher, reaching several million electron volts. A summary is given in Table II.

For comparison, we note that the highest harmonic cutoff energy, which has been attained experimentally with ordinary (helium) atoms, amounts to ≈1 keV [45]; the corresponding harmonic order at the cutoff was $\epsilon_{\max}/\omega \approx 800$. Higher cutoff energies are difficult to achieve due to the detrimental effects of dephasing [46] and electron drift motion; various schemes have been proposed to overcome this obstacle (see [19,39,47] and references therein). Muonic atoms are advantageous in this respect since the large muon mass in principle allows for the generation of million-electron-volt harmonics in the dipole regime of interaction.

TABLE II. Maximum HHG cutoff energies $\epsilon_{\max}$ achievable with hydrogenlike muonic atoms of nuclear-charge number Z. The applied laser frequency $\omega_{\min}$ and intensity parameter $\xi_{\max}$ are chosen in accordance with Eqs. (8)–(10) to allow for an efficient ionization-recollision process. $\xi_{\min}$ denotes the minimum intensity parameter leading to tunneling ionization [19].

Z	$\hbar\omega_{\min}$	$\xi_{\min}$	$\xi_{\max}$	$\epsilon_{\max}$
1	27 eV	0.007	0.085	0.55 MeV
2	170 eV	0.015	0.12	1.1 MeV
4	960 eV	0.03	0.17	2.2 MeV
10	9.5 keV	0.07	0.27	5.7 MeV

As a result, muonic atoms are promising candidates for the generation of hard x rays or even γ rays which might be employed to trigger photonuclear reactions.

B. Nuclear-mass effects

In this section, we consider the effect on the harmonic cutoff position stemming from a variation of the nuclear mass among isotopes. In a strong laser field with $U_p \gg I_p$, the harmonic cutoff position $\epsilon_{\max}$ is mainly determined by the value of the ponderomotive energy (of the relative motion). The latter is determined by the coupling of the relative coordinate to the laser field and exhibits a dependence on nuclear parameters, as an inspection of Eq. (3) shows.

For muonic hydrogen isotopes, the ponderomotive energy of the relative motion reads

$$U_p = \frac{e^2 E^2}{4\omega^2 m_r} = \frac{e^2 E^2}{4\omega^2} \left(\frac{1}{m_\mu} + \frac{1}{m_n} \right) \tag{11}$$

and is, thus, larger as the reduced mass becomes smaller. Consequently, in an intense laser field with $U_p \gg I_p$, muonic hydrogen (H) will give rise to a larger cutoff energy than muonic deuterium (D). The relative difference is about 5% according to $\epsilon_{\max}^{(\mathrm{H})}/\epsilon_{\max}^{(\mathrm{D})} \approx m_r^{(\mathrm{D})}/m_r^{(\mathrm{H})} \approx 1.05$. Note that $m_r^{(\mathrm{H})} \approx 0.90 m_\mu$, whereas $m_r^{(\mathrm{D})} \approx 0.95 m_\mu$.

The difference in the cutoff positions due to the nuclear-mass effect can also be understood more intuitively within the two-particle picture, instead of the relative motion. The right-hand side of Eq. (11) describes a ponderomotive energy that consists of two parts: one for the recolliding muon and one for the recolliding nucleus. The total pondermotive energy is thus a sum of the ponderomotive energies of the muon and the nucleus. Both particles are driven into opposite directions by the laser field, and when they recollide, their kinetic energies add up. In this picture, the higher cutoff energy of the hydrogen atom arises from the larger ponderomotive energy of the proton as compared to the heavier deuteron.

For higher nuclear-charge numbers ($Z > 1$), the ponderomotive energy of the relative motion differs from Eq. (11). The laser-driven dynamics of the muon-nucleus system becomes more complex then, which is reflected in the effective muon charge being different from unity ($q_e > e$). Hence, in the general case, we obtain from Eq. (3) the ponderomotive energy of the relative motion

$$U_p^{(Z)} = \frac{q_e^2 E^2}{4\omega^2 m_r} = \frac{e^2 E^2 m_r}{4\omega^2} \left(\frac{Z}{m_n} + \frac{1}{m_\mu} \right)^2, \tag{12}$$

which reduces to Eq. (11) for $Z = 1$. It is interesting to observe that Eq. (12), in contrast to Eq. (11), does not simply separate into a sum of the ponderomotive energies of the muon and the nucleus; that is, it is different from $U_p' \equiv (e^2 E^2/4\omega^2)(Z^2/m_n + 1/m_\mu)$. The reason is that in the case of $Z > 1$, the center of mass does not stay at rest. Rather, the ponderomotive energy $U_p^{(\mathrm{cm})} \equiv (Z-1)^2 e^2 E^2/4\omega^2 M$ is connected with its motion. The relation between the various ponderomotive energies is

$$U_p' = U_p^{(Z)} + U_p^{(\mathrm{cm})}. \tag{13}$$

Only in the case of hydrogen isotopes ($Z = 1$) does the center-of-mass coordinate remain at rest since the total charge

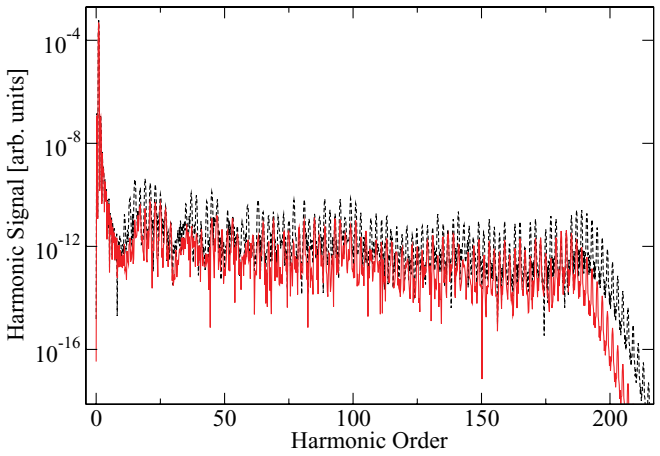

FIG. 1. (Color online) HHG spectra for muonic hydrogen (dashed black line) and deuterium [solid grey (red) line], respectively. The laser parameters are $I = 1.05 \times 10^{23}$ W/cm^2 and $\hbar\omega = 118$ eV, corresponding to $\xi \approx 0.02$. The calculation was performed in one spatial dimension using the soft-core potential (14).

is zero, so that $U_p^{(\mathrm{cm})} = 0$ and $U_p^{(Z=1)}$ [see Eq. (11)] fully accommodates the single-particle ponderomotive energies.

As an illustration, Figs. 1 and 2 show numerically calculated HHG spectra for muonic hydrogen and helium isotopes exposed to very intense laser fields of high frequency. They were produced by solving the TDSE (3) in one spatial dimension via the Crank-Nicolson time-propagation scheme. The muon-nucleus interaction is modeled by a soft-core potential

$$V_s(x) = -\frac{Ze^2}{\sqrt{x^2 + a^2}}, \tag{14}$$

with the Bohr radius $a = \rho a_0/Z$ of the muonic atom; a_0 denotes the usual Bohr radius of the electronic ground state of hydrogen. The potential (14) results from the standard soft-core potential $V(x_e) = -e^2/\sqrt{x_e^2 + a_0^2}$ [48] by applying the scaling transformation of Eq. (5). Note that the precise shape

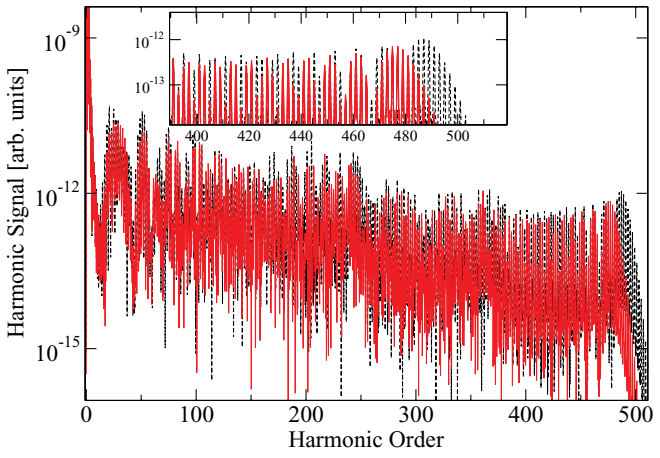

FIG. 2. (Color online) HHG spectra for muonic ^{3}He (dashed black line) and ^{4}He [solid grey (red) line], respectively, at the laser parameters $I = 8 \times 10^{24}$ W/cm^2 and $\hbar\omega = 347$ eV. The inset shows an enlargement of the cutoff region.

of the binding potential is immaterial for the position of the harmonic cutoff as long as $U_p \gg I_p$. The laser field has been chosen as a five-cycle pulse of trapezoidal envelope having one cycle for linear turn on and one for turn off. The HHG spectrum is obtained from a Fourier transformation of the dipole acceleration.

Figure 1 shows the harmonic spectra for muonic hydrogen (where the nucleus is a proton) versus muonic deuterium. In accordance with Eq. (11), for muonic hydrogen the spectrum extends further including five more (odd) harmonics as compared with that of deuterium, corresponding to an increase of the cutoff position by 5%. Besides, a relative enhancement of the spectral plateau height is found. The difference between the cutoff positions increases to about sixty harmonics, when the applied frequency is reduced to 59 eV (see Fig. 1 in [16]).

In Fig. 2, the harmonic spectra for different muonic helium isotopes in an ultraintense, soft x-ray laser field are shown. The spectrum for ^{3}He extends further by ten more harmonics in contrast with that of ^{4}He. We point out that formula (11), which holds for hydrogen atoms ($Z = 1$) and takes into account only the different reduced masses, would predict a difference of only five harmonics for this case. The general formula (12), however, correctly predicts the difference in the cutoff positions in Fig. 2. Hence, we see that the effective muon charge can have a measurable impact on the HHG response.

C. Nuclear-size effects

In this section, we study the influence of the nuclear extension on the harmonic spectra from muonic atoms. While the impact of the nuclear mass on the cutoff position followed from analytical considerations in Sec. III B, our investigation of nuclear-size effects will rely on numerical solutions of the TDSE (3) and a comparative study of the radiative responses from different muonic isotopes.

The softcore potential (14), which has been applied in Figs. 1 and 2 and which is very common in strong-field physics, is not suitable to incorporate a finite nuclear extension. Instead, we apply for this purpose the nuclear drop model and consider the nucleus as a sphere of uniform charge density within the nuclear radius R. The corresponding potential, restricted to one dimension, reads

$$V_h(x) = \begin{cases} -\frac{Ze^2}{R}\left(\frac{3}{2} - \frac{x^2}{2R^2}\right) & \text{if } |x| \leqslant R, \\ -\frac{Ze^2}{|x|} & \text{if } |x| > R, \end{cases} \tag{15}$$

which explicitly takes the nuclear radius into account. We point out that in the limit $R \to 0$, the binding energy of the lowest lying state of this potential becomes infinite and, thus, unphysical [49]. Following a well-established procedure [49–51], we therefore start our calculations from the first excited state, which has the correct binding energy. By monitoring the projection onto the unphysical state during the time evolution, we take care that the occupation of this state always stays negligibly small.

The dimensional reduction of the problem clearly represents an approximation which, however, is indicated for reasons of computational feasibility. We note that even the one-dimensional (1D) numerics is a nontrivial task in our

case because of the fine grid spacing required to resolve the nuclear extension and the nonstandard laser parameters employed; with regard to ordinary atoms, the latter would correspond to intense fields in the midinfrared region, giving rise to large muon momenta and ponderomotive energies. As a consequence of the approximate approach, the following discussion is more qualitative in nature (contrary to the preceding sections).

Two isotopes with different radii also differ in mass. It is useful to separate the impact of the nuclear size on the HHG process from the nuclear-mass effect, which was discussed in the previous section. To this end, we compare HHG spectra from different isotopes where the nuclear-mass effect has been removed by a suitable adjustment of the laser frequencies and intensities. In accordance with the scaling relations (7), this was achieved by applying the scaled parameters $\omega \propto m_r$ and $E \propto m_r^2/q_e$ (at a given value of Z). In this manner, the laser-driven muonic isotopes become equivalent to the same ordinary hydrogen atom, with the only difference being the size of the binding nucleus. In particular, the harmonic cutoff positions are forced to coincide this way. [Note that the application of either potential (14) or (15) gives rise to the same harmonic cutoff position.]

We start with the calculations for muonic hydrogen and deuterium shown by Fig. 3. As mentioned previously, in order to avoid residual signatures from the nuclear-mass effect we apply the laser parameters $I^{(\mathrm{H})} = 1.05 \times 10^{23}$ W/cm^2 and $\hbar\omega^{(\mathrm{H})} = 177$ eV to muonic hydrogen, whereas muonic deuterium is subject to the parameters $I^{(\mathrm{D})} = 1.30 \times 10^{23}$ W/cm^2 and $\hbar\omega^{(\mathrm{D})} = 186$ eV. The harmonic signal from muonic hydrogen is larger (by about 50% in the cutoff region) than that from muonic deuterium. The reason is that in the case of muonic hydrogen the nuclear radius is smaller, which generates a steeper potential near the origin (see Fig. 4). This leads to a larger potential gradient in this region,

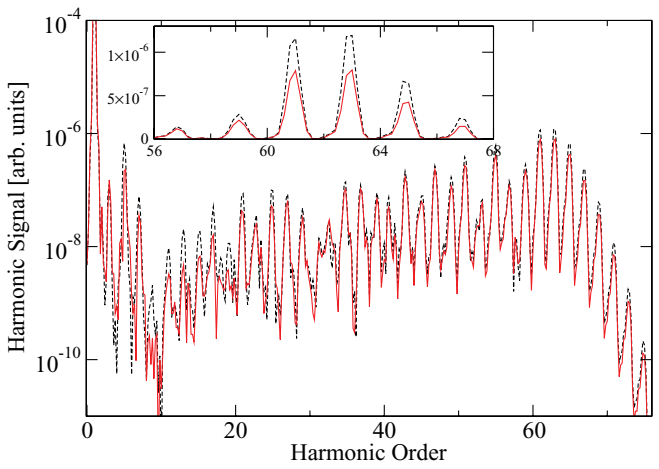

FIG. 3. (Color online) HHG spectra calculated with the hardcore potential (15). The dashed black line represents the spectrum for muonic hydrogen at the laser parameters $I^{(\mathrm{H})} = 1.05 \times 10^{23}$ W/cm^2 and $\hbar\omega^{(\mathrm{H})} = 177$ eV. The solid grey (red) line represents the spectrum for muonic deuterium at the appropriatly scaled laser parameters $I^{(\mathrm{D})} = 1.30 \times 10^{23}$ W/cm^2 and $\hbar\omega^{(\mathrm{D})} = 186$ eV in order to compensate for the nuclear-mass effect. The inset shows an enlargement of the cutoff region on a linear scale.

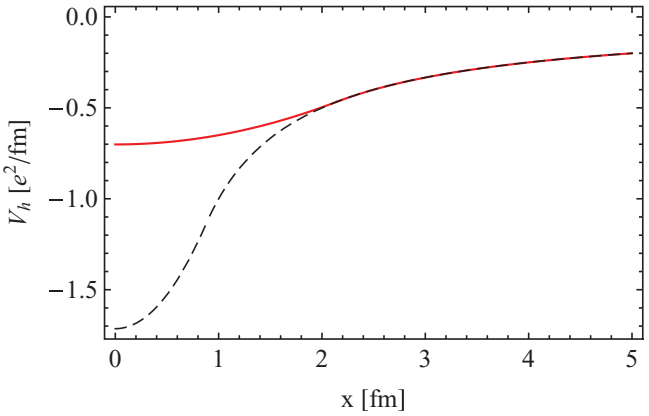

FIG. 4. (Color online) Inner region of the hardcore potentials generated by a proton in muonic H (dashed black line) and by a deuteron in muonic D [solid grey (red) line], according to Eq. (15).

which accelerates the atomic dipole according to Ehrenfest's theorem [52]. The muon in hydrogen is thus more strongly accelerated, leading to enhanced harmonic emission. A relative enhancement of 50% of the near-cutoff harmonics was also found at lower laser frequencies ($\omega \approx 60$ eV) at the same laser intensity [16]. We note that the relative enhancement is reduced to about 10%, when smaller laser intensities ($I \approx 4 \times 10^{22}$ W/cm^2) are applied.

In the case of muonic helium isotopes, the harmonic signal from ^{4}He is expected to be larger than that from ^{3}He. The reason is that ^{4}He is a doubly magic nucleus of very compact size (see Table I). This expectation is confirmed by Fig. 5(a), where a relative difference of about 10% in the cutoff region is observed. The fact that the difference is reduced in comparison with the muonic hydrogen isotopes can be attributed to the smaller relative difference of the nuclear radii: $R^{(^3\mathrm{He})}/R^{(^4\mathrm{He})} \approx 1.16$, whereas $R^{(\mathrm{D})}/R^{(\mathrm{H})} \approx 2.44$. On the other hand, however, the muon comes closer to the binding nucleus when the charge number Z increases, which should enhance the sensitivity to the nuclear size. This circumstance becomes important when we move on to muonic lithium ($Z = 3$). Here, the difference between the harmonic signals from muonic ^{6}Li versus muonic ^{9}Li amounts to about 20% in the cutoff region [see Fig. 5(b)], which is larger than for the helium isotopes, although the ratio of the nuclear radii $R^{(^6\mathrm{Li})}/R^{(^9\mathrm{Li})} \approx 1.14$ is similar here. In order to facilitate the comparison between helium and lithium, the laser parameters in Fig. 5 were chosen to generate a uniform cutoff position. Finally, a comparison of the radiative responses from muonic ^{20}Ne and ^{23}Ne at the corresponding field parameters reveals almost identical HHG spectra (not shown). The relative enhancement of the HHG signal from the smaller isotope ^{23}Ne as compared with ^{20}Ne is of the order of 1%. Here, the ratio of the nuclear radii, $R^{(^{20}\mathrm{Ne})}/R^{(^{23}\mathrm{Ne})} \approx 1.03$, is close to unity. We note moreover that in the cases of lithium and neon practically no mass effect needs to be compensated since the corresponding reduced muon masses almost coincide.

It is interesting to note that recent studies of recollision phenomena such as above-threshold detachment of negative ions [53] or laser-assisted potential scattering [54] have

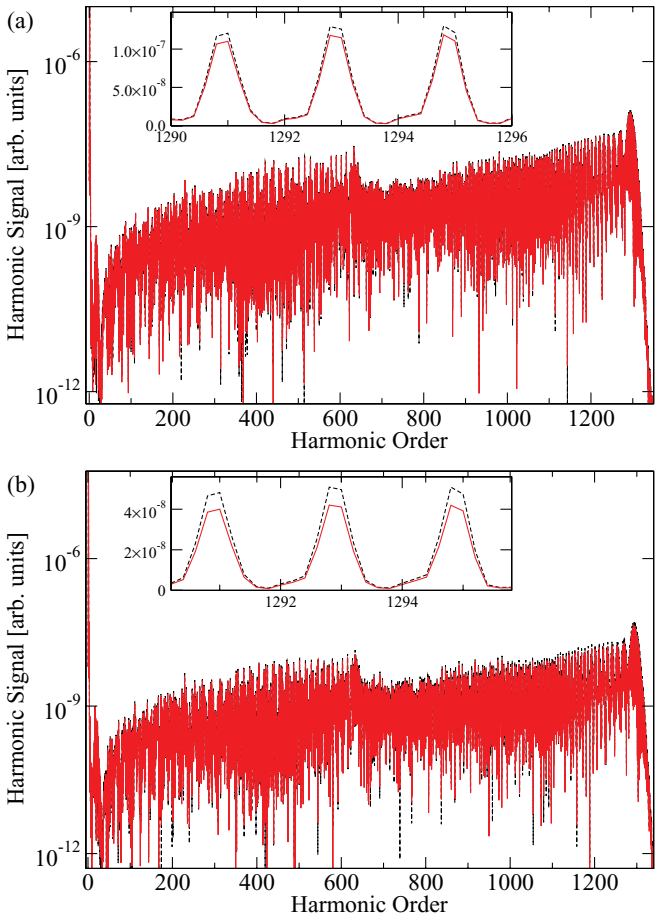

FIG. 5. (Color online) HHG spectra calculated with the hard-core potential (15). (a) The dashed black line shows the spectrum for muonic ^{4}He at the laser parameters $I^{(^4\mathrm{He})} = 8.7 \times 10^{24}$ W/cm^2 and $\hbar\omega^{(^4\mathrm{He})} = 255$ eV. The solid grey (red) line represents the spectrum for muonic ^{3}He at the accordingly scaled values $I^{(^3\mathrm{He})} = 8.3 \times 10^{24}$ W/cm^2 and $\hbar\omega^{(^3\mathrm{He})} = 253$ eV. (b) Same as (a) but for muonic ^{9}Li at $I^{(^9\mathrm{Li})} = 1.06 \times 10^{26}$ W/cm^2, $\hbar\omega^{(^9\mathrm{Li})} = 583$ eV (dashed black line) and muonic ^{6}Li at $I^{(^6\mathrm{Li})} = 1.01 \times 10^{26}$ W/cm^2, $\hbar\omega^{(^6\mathrm{Li})} = 580$ eV [solid grey (red) line].

found a relative enhancement of the rescattering probability for atomic systems of *larger* core size. For example, the rescattering contribution is more pronounced in Br^- than F^- ions [53]. The reason for the enhancement effect is similar as in the present case: The larger Br^- ion of nuclear charge $Z = 35$ creates a potential of increased depth and spatial variation as compared with the F^- ion where $Z = 9$. The nuclear extension is immaterial in these electronic systems of Angstrom dimension. In our comparative study of the harmonic yield from different hydrogenlike muonic isotopes of the same element ($Z = \mathrm{const}$), the situation only differs in the sense that here the nuclear size does play a role, with the deeper and steeper potentials arising from *smaller* nuclear isotopes of the same element.

When considering laser-driven recollisions, the de Broglie wavelength of the returning quantum wave packet can be of importance as well. In fact, for the case of ordinary molecules, it has been shown that the electron wavelength can become as small as the internuclear distance within the molecule, causing characteristic diffraction patterns [55]. In the present case of muonic atoms, a similar effect could in principle arise when the de Broglie wavelength of the recolliding muon compares with the nuclear size. However, the wavelength of a muon with a kinetic energy of a few million electron volts (see Table II) amounts to about 50 fm, which exceeds any nuclear radius substantially and thus prevents diffractive muon-nucleus scattering.

Concluding this subsection, our 1D model calculations provided evidence for characteristic nuclear-size signatures in the HHG spectra of muonic atoms: Smaller nuclear isotopes are expected to produce enhanced harmonic emission due to the larger potential depths and gradients associated with them. We point out, however, that the influence of the nuclear size might be overestimated by our 1D hardcore-potential approach as the muon meets the nucleus more often than in the real three-dimensional (3D) case. In particular, the muon's wave-packet spreading in the transversal direction is neglected, which can substantially reduce the absolute harmonic yield. One may in principle expect that the *relative* differences in the HHG spectra revealed in the present benchmark calculations are less sensitive to model assumptions than absolute numbers. Nevertheless, a future calculation in higher dimensionality would be desirable, providing more accurate quantitative predictions on the nuclear-size effect whose physical origin and basic features have been presented here.

D. Comparison with electronic systems

Finite nuclear-size effects—in the absence of any external laser field—have been revealed in high-precision spectroscopy of electron transitions in (ordinary) highly charged ions (see, e.g., [56] for recent experiments). When such ionic systems are exposed to a superintense laser field [57], nuclear signatures may be present in their high-harmonic response as well. It is of interest to compare the expected effects with those found for laser-driven muonic atoms in Sec. III C. To this end, we perform a simple analysis which is based on nonrelativistic Schrödinger theory; the relativistic electron motion in highly charged ions is ignored in this rather qualitative discussion.

We assume a hydrogenlike system of nuclear-charge number Z and employ the mass scaling parameter ρ from Eq. (5), with $\rho \approx 1/200$ for a muonic atom and $\rho = 1$ for an electronic ion. The K-shell Bohr radius, binding energy, and Coulombic field strength amount to $a_K(Z,\rho) = a_0\rho/Z$, $I_p(Z,\rho) = \epsilon_0 Z^2/\rho$, and $E_K(Z,\rho) = E_0 Z^3/\rho^2$, respectively, where a_0, ϵ_0, and E_0 denote the corresponding quantities for ordinary hydrogen. The nuclear radius can be approximated roughly as $R(Z) \approx 1.2(2Z)^{1/3}$ fm and has a typical relative variation among different isotopes of a few percents (except for hydrogen verus deuterium). Similar finite nuclear-size effects in the HHG spectra can be expected when the ratio $R(Z)/a_K(Z,\rho) \propto Z^{4/3}/\rho$ has a similar value for two atomic systems that are compared. This is the case, for example, for electronic U^{91+} (where $Z = 92, \rho = 1$) and muonic He^+ (where $Z = 2, \rho \approx 1/200$).

These relations imply, however, that the binding energy and electric field strength in the electronic ion are substantially larger than in the muonic atom when both have the same ratio of $Z^{4/3}/\rho = \mathrm{const}$. As a consequence, the laser frequency

and intensity that must be applied to the electronic highly charged ion in order to reveal finite nuclear-size effects in the harmonic response need to be larger than in the muonic atom case. Against this background, muonic atoms appear as more favorable systems than ordinary heavy ions to study the influence of the nuclear size on the HHG process.

IV. CONCLUSION AND OUTLOOK

Motivated by the sustained progress in the development of powerful laser sources, we have studied the harmonic radiation emitted by muonic atoms exposed to high-intensity, high-frequency laser fields. It was shown that maximum harmonic cutoff energies in the million-electron-volt domain can be achieved, rendering this species of exotic atoms promising candidates for the generation of (weak) ultrashort coherent γ-ray pulses which might be employed to trigger photonuclear reactions. Our results demonstrate, moreover, that strongly laser-driven muonic atoms can, in principle, be utilized to dynamically gain structure information on nuclear ground states via their high-harmonic response.

(1) On the one hand, the harmonic cutoff position extends to larger values for isotopes of smaller mass. For the hydrogen isotopes, this effect is fully explicable in terms of the reduced mass, whereas for atomic numbers $Z > 1$ an additional contribution stems from an effective muon charge which affects the relative motion generating the harmonics. (2) On the other hand, 1D model calculations provide clear indications that the harmonic signal strength additionally depends on the nuclear size, being enhanced for more compact isotopes of the same element because of the deeper and steeper potential they create. Corresponding nuclear-size effects in the high-harmonic emission from ordinary highly charged ions are expected to be less pronounced.

Furthermore, we point out that the interaction of a muonic atom with ultrastrong laser fields may lead to excitation of the nucleus. Nonresonant nuclear Coulomb excitation has recently been studied when a bound muonic wave packet is driven into coherent oscillations by an external laser field [58]; the resulting nuclear-excitation probabilities were found to be small, though. When the laser field is sufficiently strong to ionize the muon as in the HHG scenario, however, the kinetic energy gain in the continuum up to the million-electron-volt range allows for nuclear excitation upon the muon-nucleus recollision. Corresponding studies of laser-driven electron-impact excitation of the nucleus have been carried out in ordinary atoms and ions [59]. It is even conceivable to conduct pump-probe experiments on excited nuclear levels: The periodically driven muon can first excite the nucleus and then probe the excited state and its deexcitation mechanism during a subsequent encounter.

ACKNOWLEDGMENTS

We are grateful to A. Staudt for valuable discussions and for providing us with his computer code. We also thank A. D. Bandrauk, K. Z. Hatsagortsyan, C. H. Keitel, N. L. Manakov, and J. Ullrich for useful conversations. AS acknowledges support by the Higher Education Commission (HEC), Pakistan, and Deutscher Akademischer Austauschdienst (DAAD).

[1] J. M. Eisenberg and W. Greiner, *Excitation Mechanisms of the Nucleus*, Nuclear Theory Vol. 2 (North-Holland, Amsterdam, 1976); E. Borie and G. A. Rinker, Rev. Mod. Phys. **54**, 67 (1982); M. I. Eides, H. Grotch, and V. A. Shelyuto, Phys. Rep. **342**, 63 (2001).

[2] V. L. Fitch and J. Rainwater, Phys. Rev. **92**, 789 (1953).

[3] F. Mulhauser *et al.*, Phys. Rev. A **73**, 034501 (2006); for current information, see [www.triumf.info and www.psi.ch].

[4] T. Nilsson *et al.*, Nucl. Phys. A **746**, 513 (2004).

[5] J. A. Maruhn, V. E. Oberacker, and V. Maruhn-Rezwani, Phys. Rev. Lett. **44**, 1576 (1980).

[6] W. H. Breunlich and P. Kammel, Annu. Rev. Nucl. Part. Sci. **39**, 311 (1989); M. C. Fujiwara *et al.*, Phys. Rev. Lett. **85**, 1642 (2000).

[7] H. Schwoerer, J. Magill, and B. Beleites, eds., *Lasers and Nuclei* (Springer, Heidelberg, 2006); S. Matinyan, Phys. Rep. **298**, 199 (1998); K. W. D. Ledingham, P. McKenna, and R. P. Singhal, Science **300**, 1107 (2003).

[8] See, e.g., V. S. Letokhov, Sov. Phys. Usp. **30**, 897 (1987) [Usp. Fiz. Nauk. **153**, 311 (1987)]; R. Neugart, Eur. Phys. J. A **15**, 35 (2002).

[9] K. W. D. Ledingham *et al.*, Phys. Rev. Lett. **84**, 899 (2000); T. E. Cowan *et al.*, *ibid.* **84**, 903 (2000).

[10] T. Ditmire *et al.*, Nature (London) **398**, 489 (1999).

[11] D. Umstadter, J. Phys. D **36**, R151 (2003).

[12] T. J. Bürvenich, J. Evers, and C. H. Keitel, Phys. Rev. Lett. **96**, 142501 (2006); A. Pálffy, J. Mod. Opt. **55**, 2603 (2008).

[13] G. C. Baldwin and J. C. Solem, Rev. Mod. Phys. **69**, 1085 (1997).

[14] M. Klaiber, K. Z. Hatsagortsyan, and C. H. Keitel, e-print arXiv:0707.2900v1 [physics.atom-ph].

[15] A. Ipp, C. H. Keitel, and J. Evers, Phys. Rev. Lett. **103**, 152301 (2009).

[16] A. Shahbaz, C. Müller, A. Staudt, T. J. Bürvenich, and C. H. Keitel, Phys. Rev. Lett. **98**, 263901 (2007).

[17] D. B. Milošević, G. G. Paulus, D. Bauer, and W. Becker, J. Phys. B **39**, R203 (2006).

[18] A. Scrinzi, M. Y. Ivanov, R. Kienberger, and D. M. Villeneuve, J. Phys. B **39**, R1 (2006).

[19] Y. I. Salamin, S. X. Hu, K. Z. Hatsagortsyan, and C. H. Keitel, Phys. Rep. **427**, 41 (2006).

[20] Further aspects of HHG which have recently been studied may be found, e.g., in Z. Zhao, J. Yuan, and T. Brabec, Phys. Rev. A **76**, 031404(R) (2007); A. L. Lytle, X. Zhang, J. Peatross, M. M. Murnane, H. C. Kapteyn, and O. Cohen, Phys. Rev. Lett. **98**, 123904 (2007); S. Baker *et al.*, *ibid.* **101**, 053901 (2008); S. V. Popruzhenko, M. Kundu, D. F. Zaretsky, and D. Bauer, Phys. Rev. A **77**, 063201 (2008); Z. Zhou and J. Yuan, *ibid.* **77**, 063411 (2008).

[21] S. Chelkowski, A. D. Bandrauk, and P. B. Corkum, Phys. Rev. Lett. **93**, 083602 (2004).

[22] M. Kalinski, Laser Phys. **15**, 1367 (2005).

[23] Y. Xiang *et al.*, J. Mod. Opt. **57**, 385 (2010).

[24] V. Yanovsky *et al.*, Opt. Express **16**, 2109 (2008).

[25] See, e.g., the proposal on the extreme-light infrastructure (ELI) available at [http://www.eli-laser.eu].

[26] W. Ackermann *et al.*, Nat. Photon. **1**, 336 (2007); A. A. Sorokin, S. V. Bobashev, T. Feigl, K. Tiedtke, H. Wabnitz, and M. Richter, Phys. Rev. Lett. **99**, 213002 (2007).

[27] M. Hoener *et al.*, Phys. Rev. Lett. **104**, 253002 (2010).

[28] A. Pukhov, Nature Phys. **2**, 439 (2006); G. D. Tsakiris *et al.*, New J. Phys. **8**, 19 (2006); B. Dromey *et al.*, Nature Phys. **5**, 146 (2009).

[29] V. I. Ritus, Trudy FIAN **111**, 5 (1979) [J. Rus. Laser Res. **6**, 497 (1985)]; D. A. Dicus, A. Farzinnia, W. W. Repko, and T. M. Tinsley, Phys. Rev. D **79**, 013004 (2009).

[30] We note that this is contrary to the case of two-electron atoms, where the light field interacts with the center-of-mass coordinate of the two electrons [see C. Ruiz, L. Plaja, L. Roso, and A. Becker, Phys. Rev. Lett. **96**, 053001 (2006)].

[31] L. B. Madsen and P. Lambropoulos, Phys. Rev. A **59**, 4574 (1999).

[32] H. R. Reiss, Phys. Rev. A **19**, 1140 (1979).

[33] A. D. Bandrauk, O. F. Kalman, and T. T. Nguyen Dang, J. Chem. Phys. **84**, 6761 (1986).

[34] J. W. Rohlf, *Modern Physics from* α *to* Z^0 (Wiley, New York, 1994).

[35] P. J. Mohr and B. N. Taylor, Rev. Mod. Phys. **77**, 1 (2005).

[36] I. Angeli, At. Data Nucl. Data Tables **87**, 185 (2004).

[37] R. Sánchez *et al.*, Phys. Rev. Lett. **96**, 033002 (2006).

[38] R. C. Nayak and L. Satpathy, At. Data Nucl. Data Tables **73**, 213 (1999).

[39] K. Z. Hatsagortsyan *et al.*, J. Opt. Soc. Am. B **25**, B92 (2008).

[40] S. Palaniyappan, I. Ghebregziabher, A. DiChiara, J. MacDonald, and B. C. Walker, Phys. Rev. A **74**, 033403 (2006).

[41] M. V. Frolov, A. V. Flegel, N. L. Manakov, and A. F. Starace, Phys. Rev. A **75**, 063408 (2007); M. V. Frolov, N. L. Manakov, and A. F. Starace, Phys. Rev. Lett. **100**, 173001 (2008).

[42] J. Tate, T. Auguste, H. G. Muller, P. Salieres, P. Agostini, and L. F. DiMauro, Phys. Rev. Lett. **98**, 013901 (2007); K. D. Schultz *et al.*, J. Mod. Opt. **54**, 1075 (2007).

[43] K. Schiessl, K. L. Ishikawa, E. Persson, and J. Burgdörfer, Phys. Rev. Lett. **99**, 253903 (2007).

[44] M. V. Frolov, N. L. Manakov, T. S. Sarantseva, M. Y. Emelin, M. Y. Ryabikin, and A. F. Starace, Phys. Rev. Lett. **102**, 243901 (2009).

[45] J. Seres *et al.*, Nature **433**, 596 (2005).

[46] S. L. Voronov, I. Kohl, J. B. Madsen, J. Simmons, N. Terry, J. Titensor, Q. Wang, and J. Peatross, Phys. Rev. Lett. **87**, 133902 (2001).

[47] V. D. Taranukhin, Laser Phys. **10**, 330 (2000); C. C. Chirilă, N. J. Kylstra, R. M. Potvliege, and C. J. Joachain, Phys. Rev. A **66**, 063411 (2002); M. Klaiber, K. Z. Hatsagortsyan, and C. H. Keitel, *ibid.* **74**, 051803(R) (2006); **75**, 063413 (2007).

[48] J. Javanainen, J. H. Eberly, and Q. Su, Phys. Rev. A **38**, 3430 (1988).

[49] U. Schwengelbeck and F. H. M. Faisal, Phys. Rev. A **50**, 632 (1994).

[50] I. P. Christov, J. Zhou, J. Peatross, A. Rundquist, M. M. Murnane, and H. C. Kapteyn, Phys. Rev. Lett. **77**, 1743 (1996).

[51] A. Gordon, R. Santra, and F. X. Kärtner, Phys. Rev. A **72**, 063411 (2005).

[52] The importance of the analytical behavior of the potential near the origin for the HHG process in ordinary atoms has been studied in Ref. [51].

[53] A. Gazibegović-Busuladžić, D. B. Milošević, and W. Becker, Phys. Rev. A **70**, 053403 (2004); A. Gazibegović-Busuladžić, D. B. Milosevic, W. Becker, B. Bergues, H. Hultgren, and I. Y. Kiyan, Phys. Rev. Lett. **104**, 103004 (2010).

[54] A. Čerkić and D. B. Milošević, Phys. Rev. A **70**, 053402 (2004).

[55] T. Zuo, A. D. Bandrauk, and P. B. Corkum, Chem. Phys. Lett. **259**, 313 (1996).

[56] H. Bruhns, J. Braun, K. Kubicek, J. R. Lopez-Urrutia, J. Crespo, and J. Ullrich, Phys. Rev. Lett. **99**, 113001 (2007); C. Brandau *et al.*, *ibid.* **100**, 073201 (2008).

[57] HHG from highly -charged ions has been studied, e.g., in S. X. Hu and C. H. Keitel, Phys. Rev. A **63**, 053402 (2001); M. Casu and C. H. Keitel, Europhys. Lett. **58**, 496 (2002); S. X. Hu, A. F. Starace, W. Becker, W. Sandner, and D. B. Milošević, J. Phys. B **35**, 627 (2002); C. C. Chirilă, C. J. Joachain, N. J. Kylstra, and R. M. Potvliege, Phys. Rev. Lett. **93**, 243603 (2004).

[58] A. Shahbaz, C. Müller, T. J. Bürvenich, and C. H. Keitel, Nucl. Phys. A **821**, 106 (2009).

[59] G. R. Mocken and C. H. Keitel, J. Phys. B **37**, L275 (2004); N. Milosevic, P. B. Corkum, and T. Brabec, Phys. Rev. Lett. **92**, 013002 (2004); M. Verschl and C. H. Keitel, J. Phys. B **40**, F69 (2007); A. S. Kornev and B. A. Zon, Laser Phys. Lett. **4**, 588 (2007).